Permanent-Magnetically Amplified Brake Mechanism Compensated and Stroke-Shortened by a Multistage Nonlinear Spring

Tori Shimizu, *Graduate Student Member, IEEE*, Kenjiro Tadakuma, *Member, IEEE*, Masahiro Watanabe, *Member, IEEE*, Kazuki Abe, *Member, IEEE*, Masashi Konyo, *Member, IEEE*, and Satoshi Tadokoro, *Fellow, IEEE*

***Abstract*—Electromagnetic (EM) brakes are widely used but consume electricity continuously to maintain their activated state. In this letter, for efficient braking and idling of robots and vehicles, we proposed a concept of a brake mechanism using a permanent magnet for the amplification of the pressing force between brake pads, allowing for the brake torque to be steplessly regulated by a minimal external force. The prototype of the proposed mechanism was developed with a newly devised compensation spring—not the conventional conical coil springs—comprising two linear springs to shorten the pad-detaching stroke. For proof of concept, evaluation experiments based on the Japanese Industrial Standards were conducted. Both the maximum static and average dynamic friction torques increased to 161.0% and 192.9%, respectively, when identical pads of an EM brake were used for comparison. Power saving was also achieved when braking for longer than 0.43 s; the torque–energy efficiency increased by 8.7 when measured for 1.0 s, successfully revealing the effectiveness of the proposed principle. Further, based on the force–displacement characteristic of the compensated magnet, the theoretical response time was numerically analyzed as 13.6 ms—comparable to the contrasted EM brake—validating the actual behavior of 14.0 ms.**

***Index Terms*—Actuation and joint mechanisms, force control, mechanism design.**

I. Introduction

ELECTRIC brakes are used in various mechanisms to control the speed of motion. Because they do not require large and heavy external power sources such as hydraulic or pneumatic pumps, EM brakes are favored for machines with strict limitations of volume and mass [1].

An electromagnetic brake (EM brake) is a typical example of an electric brake that engages the braking system by applying a current on the coil in the field to magnetically attract the facing ferromagnetic armature. A braking force is generated due to friction between the brake pads in these fields and the armature, although there are some different implementations: an EM track brake is used in rail vehicles that considers the rail as the armature [2]; an electric trailer brake employs rounded brake shoes pressed outwards at the drum (rotating cylinder) attached to the output axle [3]. Other EM brakes such as magnetic powder brakes and magnetorheological fluid brakes use the magnetic flux generated by the coil to bind ferromagnetic particles so that the braking torque is transmitted via shear stress from the fixed field to the output shaft [4], [5].

The EM brakes, while being compact, highly responsive, and versatile as they can be activated independent of the speed unlike dynamic brakes (which require a relative speed of the target object to be braked, and therefore, a main brake to hold it [6]), these EM brakes consume electricity to drive their coils. A long-time application of current generates an unignorable amount of Joule heat, which increases the coil resistance and thus degrades braking performance [7]. Active cooling by fans or thermoelectric coolers requires even extra power.

The abovementioned issue implies that energy-efficient EM brakes contribute to the extension of the milage of robots and vehicles with an independent power supply that has a limited capacity. This can be realized by saving energy both for sudden braking and continuous idling. Such brakes also establish the reduction of cumulative electricity cost required for robotic arms

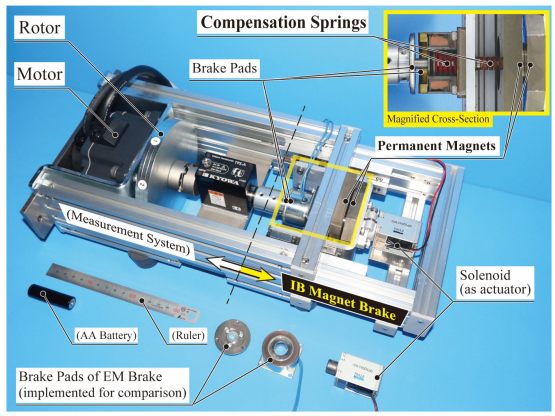

Fig. 1. Image of the proposed brake mechanism using an internally balanced magnetic unit (IBM brake) with a multistage nonlinear spring.

Manuscript received September 9, 2021; accepted January 5, 2022. Date of publication January 14, 2022; date of current version May 3, 2022. This letter was recommended for publication by Associate Editor C. Kuo and Editor C. Gosselin upon evaluation of the reviewers' comments. This work was supported in part by JSPS KAKENHI under Grant JP20J20184 and in part by Suzuki Foundation. *(Tori Shimizu and Kenjiro Tadakuma contributed equally to this work.) (Corresponding author: Kenjiro Tadakuma.)*

The authors are with the Graduate School of Information Sciences, Tohoku University, Sendai 9808579, Japan (e-mail: shimizu.tori@rm.is.tohoku.ac.jp; tadakuma@rm.is.tohoku.ac.jp; watanabe.masahiro@rm.is.tohoku.ac.jp; kazuki.abe.org@gmail.com; konyo@rm.is.tohoku.ac.jp; tadokoro@rm.is.tohoku.ac.jp).

This letter has supplementary downloadable material available at https://doi.org/10.1109/LRA.2022.3143231, provided by the authors.

Digital Object Identifier 10.1109/LRA.2022.3143231

in production lines to lock their joints intermittently. To achieve these objectives, we utilize the advantages of a permanent magnet (PM), i.e., permanent exertion of force, and thereby, the elimination of the volume and mass of the power supply. Similarly, a few existing EM brakes adopt an "electro-permanent magnet (EPM)" structure that reverses the engaging state relative to the current input. The magnetic flux of a PM maintains the excitation of the brake, and a counter EM cancels this flux to release the brake [8]. However, because they also consume electricity to keep the brake released, both EM and EPM brakes exhibit limitations in terms of holding either the enabled or disabled state continuously.

Therefore, the study aims to develop a braking system as shown in Fig. 1 that allow for a more energy-efficient actuation of the brake pads via force amplification. Further, the effectiveness of the proposed system is verified. In contrast to previous latching EPM brakes and valves that regulate the magnetic circuit passing through the yoke [9]–[11], we actuate the magnet itself to switch between attached and detached states for directly generating a pressing force, as an application of a compensated magnetic mechanisms [12]–[14]. This method is advantageous in that its output is not digital (on and off) when continuously regulating the distance between the magnets and unique in that it would ultimately contribute to braking in any machine and tool because its means of latching include, but are not limited to, electric current in a coil, solenoid, and motor; even mechanical force and human power can be used.

The remainder of this paper is organized as follows: We briefly introduce the idea of internal force compensation of a PM in Section II, which is a core technology implemented in this research. Section III discusses the principle of the proposed magnetic brake mechanism. A more sophisticated 2nd prototype to enhance the practicality of the proposed mechanism is presented in Section IV. Experiments conducted to verify the effectiveness of the second model are presented in Section V, and the results are discussed in Section VI. Finally, Section VII presents the conclusions of this study.

II. Proposal of Principle

A. Magnetic Force Compensation

Most machines use powerful actuators and large gearboxes to exert a large force. On the contrary, we adopted the idea of force compensation to avoid affecting the compactness property of the EM brake; we compensate the operating force of an actuator by maintaining the actuated part (connected to the brake pad) at an equilibrium point of the force regardless of its displacement or orientation by applying an equal load in the opposite direction. Similar applications are the self-weight compensation for elevators, cranes, and robotic arms matches the change in the potential energy of the actuated part with that of the counterweight so that they can be actuated by a considerably smaller external force [15], [16].

A mechanism known as an "internally balanced magnetic unit (IB magnet)" was invented to compensate for the magnetic potential [17]. As illustrated in Fig. 2, it comprises an attraction magnet held by the control rod and a nonlinear spring for internal balancing using both the control rod and outer frame. The spring is designed such that it has a force-displacement repulsion characteristic F_{r} that is identical, but opposite in sign, to the magnetic attraction characteristic $F_{\mathrm{m}} = -F_{\mathrm{r}}$ that increases nonlinearly with proximity to the attracted surface.

Therefore, the sum of these forces exerted on the control rod $F_{\mathrm{inter}} = F_{\mathrm{r}} + F_{\mathrm{m}}$ is canceled out. An ideally zero control force

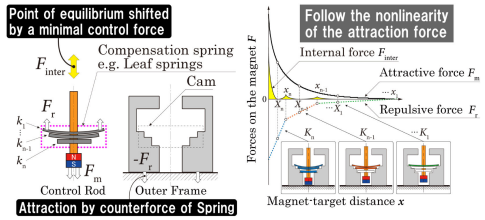

Fig. 2. Principle diagram of IB magnet. The conventional nonlinear spring is composed of multiple linear springs that work in a stepwise manner.

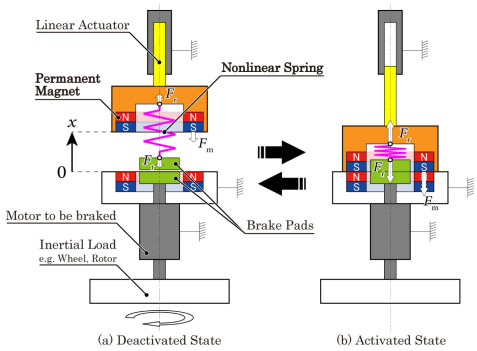

Fig. 3. Principle diagram of IBM brake. Gaps between the brake pads are exaggerated.

is required to shift the control rod to attach and detach the magnet because the control rod is then at the equilibrium point of force at any displacement x from the target object. Further, the entire mechanism is attracted to the target object by the counterforce of the F_{r} exerted on the outer frame.

B. Mechanism Principle

The IB magnet has been applied to various robotic devices such as magnetic wheels [18], magnetic crawlers [19], anchors for dangling to ceilings [20], and a connection unit for modular robots [21] because it drastically reduces the external force to control a strong PM. However, current applications have been limited to attraction mechanisms. This study is different and unique in that it generalizes the attraction motion to an indirect generation of surface pressure.

Regarding the IB magnet as a reduction mechanism, we propose a concept of the IBM brake mechanism illustrated in Fig. 3. The outer frame of the IB magnet is identified as the active brake pad driven indirectly by an actuator via the compensation spring. The ferromagnetic surface fixed on the mechanism structure (here, a magnet that faces its pole to the unlike pole of the active magnet on the control rod) attracts the control rod such that the active pad approaches the counterpart pad installed on the rotation axle to be braked. This mechanism can be considered topologically equivalent to a nonmagnetic parallel gripper reinforced by IB magnet devised in our previous study [14], which extends the outer frame as an active finger to grasp an object between a pair of IB magnets, while the proposed brake has a further sophisticated structure as the adjustment feature of the clamp width is omitted.

The spring for compensation has two roles: 1) It is a method for storing the attraction work of a magnet as elastic energy and minimizing the load on the actuator by assisting it with repulsion work when the control rod is pulled out to detach the magnet. 2) It works as a variable stiffness material that defines the internal

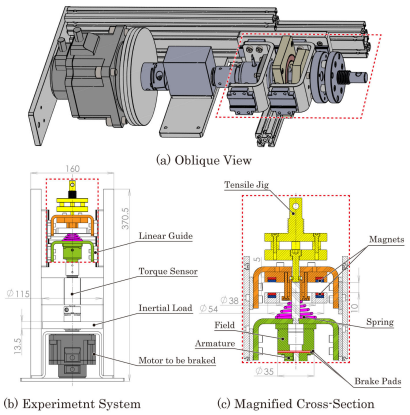

Fig. 4. Design sketch of the 1st prototype of the IBM brake. Some parts and details are omitted for better visibility. The colors of the components correspond to those of the elements in the principle diagram shown in Fig. 3.

TABLE I
SPECIFICATIONS OF THE 1ST PROTOTYPE OF THE IBM BRAKE, EM BRAKE FOR COMPARISON, AND MOTOR FOR DRIVING THE LOAD

	Components	Mass
IBM Brake with **Conical Coil Spring**	*Mass of Magnet*	40.8 [g]
	Spring	11.1 [g]
	Control Rod	405.0 [g]
	Active Brake Pad	291.7 [g]

EM Brake **AMB2.5**	*Power Rating*	3 [W] at 24 [V]
	Responsiveness	10 [ms]
Motor **BXM5120-A2**	*Rotor Inertia*	2.15 e-3 [kg·m²]
	Rated Torque	0.4 [N·mm] (continuous)
		0.8 [N·mm] (continuous)

rigidity of the brake pad by adjusting its compression width from the free length.

III. PROOF OF PRINCIPLE

A. First Prototype Model

Fig. 4 shows the dimensions of the 1st prototype of the proposed IBM brake for the proof of principle (POC), embedded in a measurement system specified in the Japanese Industrial Standard for EM brakes [22]. The brake pads of an EM brake (Ogura Clutch, AMB2.5) are diverted to those of the IBM brake such that the translational contact force between these pads becomes the single variable that affect the performance comparison of their friction torques. This measurement system can test the EM brake by screwing its field to the mechanism structure. The specifications of the contrasted brakes are listed in Table I.

As shown in Fig. 2, a conventional nonlinear spring for the IB magnet comprises multiple linear springs that activate stepwise. However, springs with different spring constants are required to duplicate the nonlinear characteristic of the magnetic attraction more precisely, which results in a bulky and heavy constitution [23]. Therefore, we utilize the nature of a conical coil spring with a varying diameter and pitch to achieve miniaturization such that its part with a smaller spring constant becomes compressed first, followed by the part with a larger spring constant [21], [24]; this nonlinearly increases its displacement–force characteristic similar to a like-pole pair of magnets by only a single elastic body.

B. Experiments for Proof-of-Concept

Using the 1st prototype, an experiment to measure the forces exerted by each component of the brake is conducted to verify the proposed principle whether a control force F_c required to detach the magnets (and the brake pads) can be reduced by the compensation provided via the nonlinear spring. The system

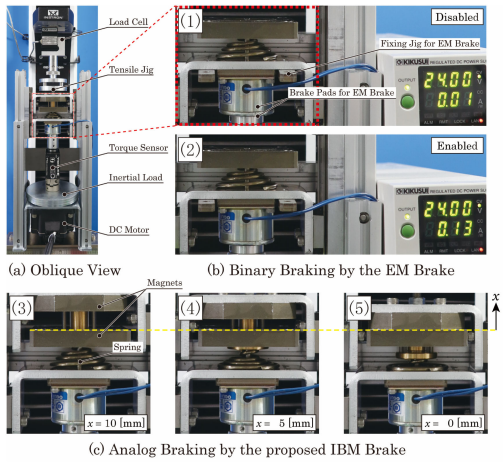

Fig. 5. Experimental system of 1st prototype of IBM brake and its operation procedure. (b) Field of EM brake pulls armature on the axle of the motor by electromagnetic attraction. (c) Pad on the field is pressed on the armature directly by the spring and indirectly by the control rod connected to the tensile jig of the material testing machine.

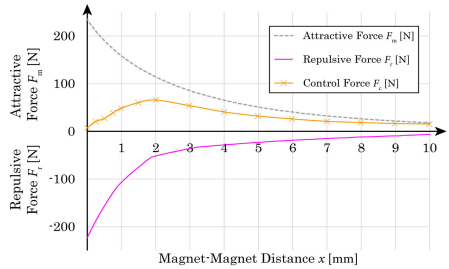

Fig. 6. Five-time average forces exerted on the control rod of the IBM brake.

constituents and experimental procedure are shown in Fig. 5, wherein a material testing machine (Instron 3343) actuates the control rod of the IB magnet with both the magnets and the spring; the magnets only; and the spring only. The respective control force F_c, single attractive force F_m, and single repulsive force F_r are recorded as shown in the graph in Fig. 6. Likewise, the attractive force between the armature and field of the excited EM brake is measured after fixing the field on the mechanism body of the experimental system.

In the abovementioned experiment, another measurement using a torque sensor (Kyowa Electronic Instruments, TPS-A-2 NM) is conducted to evaluate the relationship between the previously recorded forces and the friction torques of the proposed IBM brake and EM brake for comparison. While the position x of the control rod (distance between magnets) is kept by the material testing machine, the command value of the velocity to a brushless motor (Oriental motor, BXM5120-A2) is gradually increased so that the maximum static friction torque, i.e., the spike torque observed when the motor-driven axle starts to slip against the brake, can be measured as shown in Fig. 7.

Fig. 8 shows the results of the measurement of the maximum static friction torque, stacked in Fig. 6. As the magnets approach each other, the repulsive force of the spring steplessly increases and so does the pressing force (counterforce of spring force) between the brake pads. This leads to a continuous increase in the friction torque between the brake pads, whereas the control force remains smaller than the pressing force. Comparing the integration of F_c and F_m in range $0 \leq x \leq 10$ reveals that the

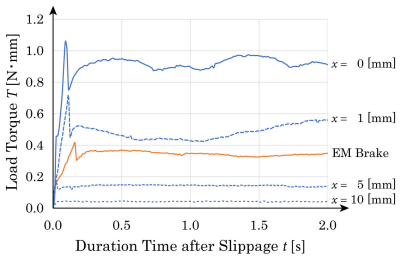

Fig. 7. Typical transitions of the friction torque of the IBM brake vary with the magnet–magnet distance (or compression distance of spring) when the axle driven by the motor begins to slip.

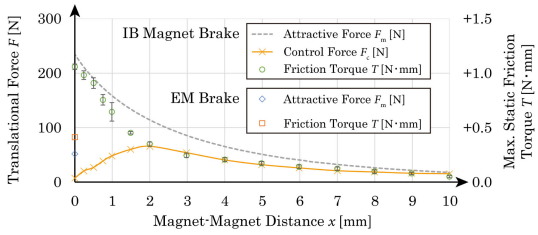

Fig. 8. Ten-time average maximum static friction torques exerted between the brake pads appended to the upper half part of Fig. 6. The values of the EM brake are depicted on the F-axis for convenience because they do not have a controllable pad–pad distance.

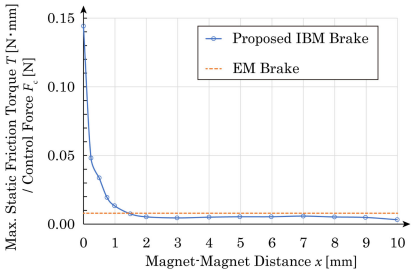

Fig. 9. Ratio of the maximum static friction torque to the control force required to sustain the current magnet–magnet distance x. The value of the EM brake is depicted as a dotted line for the same reason as in Fig. 8.

spring compensation lessened the control work required to disable the brake by 53.9% (further analyzed in Section V-A).

The ratio of the friction torque to the control force (required to maintain the current position of the control rod) is compared in Fig. 9. The value of the proposed IBM brake is comparable to but less than that of the EM brake in the range of $1.5\ \text{mm} < x$; however, it increases steeply as x approaches zero, where the torque–force ratio is more than 18.1 times that of the EM brake. This occurs because the positive correlation of the torque is established not with F_c but with the magnetic attractive force.

These results successfully prove the continuous force amplification effect by the compensation on the control force, and it indicates that a considerably weaker, smaller, and less power-consuming actuator can be chosen to drive the strong PM of the proposed IBM brake.

IV. For Higher Practicability

A. Problems of Previous Compensation Mechanism

While proven to be effective in reducing the control force, the IBM brake has a peculiar inconvenience: the control rod needs to be pulled out for a large distance to sufficiently weaken the pressing force (more than 10 mm in the current constitution),

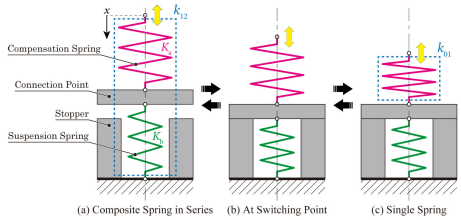

Fig. 10. Principle diagram of multistage nonlinear spring composed of two linear springs.

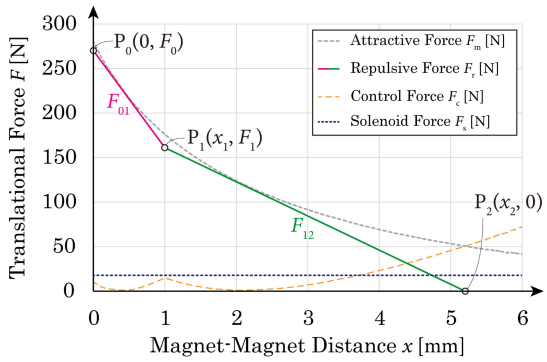

Fig. 11. Characteristic design of devised multistage nonlinear spring ($x_\text{s} = 1.5$ mm) is composed of two linear springs for the 2nd prototype of the proposed IBM brake.

although the brake pads that actually matter must be just slightly separated to deactivate braking. This side effect of compensation with an apparent reduction rate emerged because the spring transmits the attractive force of the magnets to the brake pads as long as the spring is in contact with both the control rod and the outer frame of the IB magnet.

Further, the conical coil spring itself has a problem in production; its characteristic was adjusted to follow that of the magnetic attraction on every millimeter by rectifying the pitch and diameter, which results in a long lead time. Its size and shape are uncontrollable if the compensation precision is prioritized; therefore, the structural design of the brake is strongly limited by the spring. These features are unfavorable for ensuring the flexibility of the mechanism design for mass production, where each pair of magnets has its own attractive characteristic for the spring to follow. Even magnets of identical models and lot numbers have differences in their magnetization quality, as seen when comparing Figs. 8 and 11.

B. Development of Multistage Nonlinear Spring

The brake pads should be separated in an actuation stroke as short as possible to solve the travel distance problem of the control rod. However, simply inserting a suspension spring between them affects the characteristics of the compensation spring, and this results in an excess repulsive force that hinders the activation motion of the brake.

Therefore, the 2nd prototype adopts a newly devised nonlinear spring composed of two linear springs that realizes both the early separation of the brake pads and the simplicity of design by exploiting the existence of that suspension spring. As illustrated in Fig. 10, the compensation spring K_a and suspension spring K_b are combined in series such that (a) around the free length, they work as a single elastic body with a smaller spring constant k_{12}

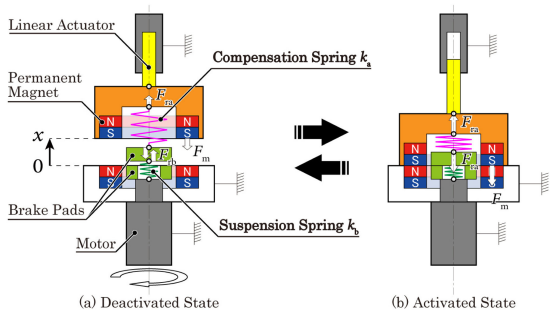

Fig. 12. Principle diagram of the 2nd prototype of the IBM brake using devised multistage spring composed of two linear springs.

represented by

$$k_{12} = \left(\frac{1}{K_\mathrm{a}} + \frac{1}{K_\mathrm{b}}\right)^{-1} = \frac{K_\mathrm{a}K_\mathrm{b}}{K_\mathrm{a}+K_\mathrm{b}} \tag{1}$$

As the combined spring k_{12} is compressed, (b) the stopper located at the switching point P_1 touches the connection point of the springs and inhibits further movement of K_b. (c) The multistage spring then has $k_{01} = K_\mathrm{a}$ as the only deformable body, which results in increased spring constant. This constitution is similar to the use of a top-out spring for a vehicle, supplementarily added to the main suspension spring in series to react to both large bumps and small vibrations by changing its spring constant based on the compressed length [25].

In this way, the brake pads can be separated in a stroke that is considerably smaller than a single conical coil spring. In exchange, the pressing force applied on the pads by K_a is predicted to be weakened by the internal force generated by K_b, which results in a decrease in the friction torque to some extent. The apparent reduction rate still exists in this manner.

The spring characteristic was designed, and the linear springs to be combined were selected in the following procedure. First, three temporal points $\mathrm{P}_0(0,\ F_0)$, $\mathrm{P}_1(x_1,\ F_1)$, and $\mathrm{P}_0(x_2,\ 0)$ defined a compensation curve F_{01} with inclination k_{01} and a suspension curve F_{12} with inclination k_{12} as

$$F_{01(x)} = -k_{01}x + b_{01} = \frac{F_1-F_0}{x_1}\,x + F_0 \tag{2}$$

$$F_{12(x)} = -k_{12}x + b_{12} = \frac{-F_1}{x_2-x_1}\,(x-x_1)\,x \tag{3}$$

Once the separation point x_1 was fixed according to the mechanism design requirement, the remaining parameters F_0, F_1, and x_2 were optimized by a numerical analysis: minimizing the integral of the control force F_c (difference between the forces F_m and F_s) for the range of compensation, i.e., control work E_c, yields the appropriate coordinates. Then, an actuator with an output force sufficient to pull out and push in the control rod for its stroke $x_\mathrm{s} > x_1$ to detach the brake pads was selected.

An example of how the multistage spring is implemented in the IBM brake is illustrated in Fig. 12. The suspension spring K_b is inserted between the active brake pad (driven indirectly by the control rod via the compensation spring K_a) and the rotation axle so that its own height can be ignored when fully compressed; the brake pads can contact each other. A thrust bearing is installed in-between to isolate the rotation and avoid friction between the axle and the spring.

C. Second Prototype Model

Fig. 13 and Table II show the dimensions and specifications of the 2nd prototype of the proposed IBM brake with a multistage spring displayed in Fig. 1 built by replacing the nonlinear spring

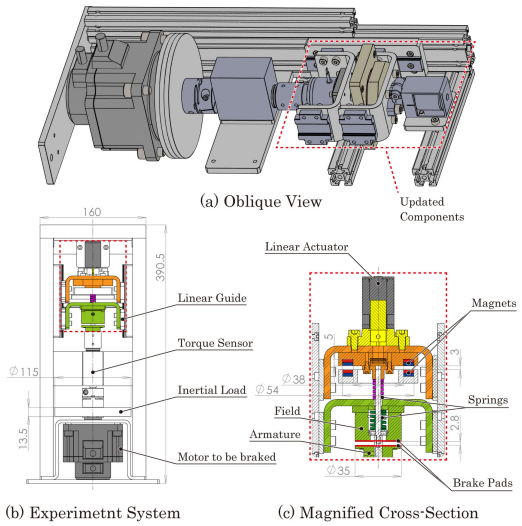

Fig. 13. Design sketch of the 2nd prototype of the IBM brake.

TABLE II
SPECIFICATION OF 2ND PROTOTYPE OF THE IBM BRAKE AND SOLENOID FOR ACTUATION

IBM Brake with **Multistage Spring**	**Components**	**Mass**	Solenoid **CD12400100**	*Power Rating*	57 [W] at 24 [V]
	Spring K_a	2.4 [g]		*Duty Cycle*	6 [%]
	Spring K_b	5.0 [g]		*Mass*	140.6 [g]
	Control Rod	441.7 [g]		*Mass of Plunger*	26.7 [g]
	Active Brake Pad	303.0 [g]		*Self-Hold Force*	10.5 [N]

and some parts for height adjustment on the control rod from the 1st prototype.

In this study, a self-holding pull solenoid (Takaha Kiko, CD12400100) is selected to regulate the control rod as an example of a weak, short-stroke actuator (half in power and one third in mass and volume of CA16620040, for example, a pull solenoid strong enough to actuate the 1st prototype but without self-holding feature). It has the same voltage rating as the EM brake, and therefore, the difference in the measured current directly represents the difference in power consumption, which simplifies the performance comparison. Meanwhile, any translational actuator can replace the role as long as they have sufficient capability to shift the rod for the designed stroke.

This self-holding solenoid operates in the following manner. Initially, when the brake is disabled, its internal PM holds keeps the control rod pulled out even without applying a current. The current is applied to the electromagnet to cancel out the flux of the internal magnet and enable the brake. The solenoid does not have a return spring to push the rod, and therefore, the control force of the IB magnet is adjusted to be weakly biased such that the attractive force is still left after compensation and pulls in the rod automatically when the self-holding is deactivated; this results in the activation of the brake. A current in the opposite direction is applied to pull out the rod to release the brake. Brake pads are in contact as soon as the magnet on the mechanism structure and the other on the control rod are attracted to each other; therefore, the solenoid must be excited just for a moment for activation.

Fig. 14 shows a cross-sectional view of the 2nd prototype. As designed, the multistage action of the springs was observed as indicated in the pictures (1)–(3) corresponding to the states of springs in the principle diagram shown in Fig. 10(a)–(c) respectively: Two springs form a composite spring, while the field (active brake pad) is suspended in stage (1), and the suspension spring stops further compression as the brake pads meet at (2), which

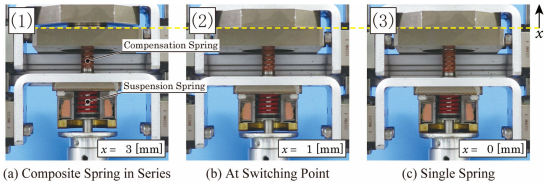

Fig. 14. Magnified cross-sectional view of the brake system of the 2nd prototype of IBM brake.

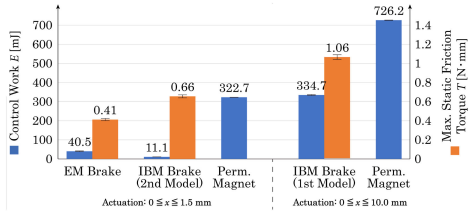

Fig. 15. Ten-time average maximum static friction torques exerted between the brake pads and the five-time average control works required to actuate the brakes for their designed maximum strokes.

results in the activation of the single action of the compensation spring as seen in (3).

V. Evaluation Experiments

A. Experiment 1: Comparison of Static Braking Torque

To investigate the property of the 2nd prototype in the same way as the experiments in Section III, its maximum static friction torque at magnet–magnet (pad–pad for EM brake) distance $x = 0$ and control force in the range of $0 \leq x \leq 1.5$ mm were measured and integrated with respect to x to derive the control work required for disabling the brake.

The results are shown in Fig. 15 with the values of the 1st prototype, indicating that the multistage spring is also valid for nonlinear compensation. Although the attractive force of PMs in the 2nd prototype is so strong that its control work E_{m} required for an actuator to fully pull out the control rod is 796.8% of that of the EM brake E_{EM}, the compensation reduced it to 27.4% of E_{EM}. Meanwhile, the maximum static friction torque is increased to 161.0% of that of the EM brake, which makes the torque–energy ratio 5.87 times.

Comparing the results of two prototypes clarifies effects of shortening x_{s}: E_{m} gets halved even without compensation, and the rate of reduction of E_{IBM} to E_{EM} improved from 53.9% to 96.6%. As a trade-off, the friction torque at $x = 0$ decreased by 38.1% because the contact force between the brake pads is hampered by the repulsive force of the suspension spring.

B. Experiment 2: Comparison of Dynamic Braking Torque, Power Consumption, and Responsiveness

To derive a performance index during braking of a rotating object, the dynamic characteristics of the IBM brake were inspected. The experimental system was laid horizontally so that the responsiveness is independent of the weight of the moving parts. While a constant command value was input to the motor to ensure that the motor attempts to maintain its rotation speed, the brake was activated for 1.0 s to exert its dynamic friction torque.

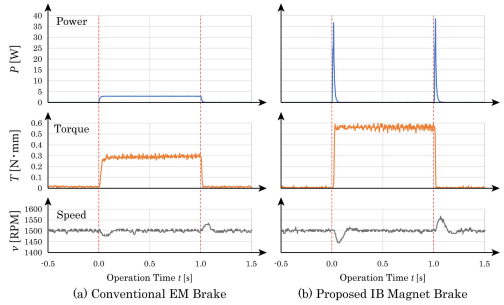

Fig. 16. Typical transitions of power consumption, friction torque, and rotation speed of the EM brake and proposed IBM brake when they braked a motor, regulated to rotate at 1500 RPM, for 1.0 s. The solenoid was excited for 14.0 ms each time the IBM brake was activated and deactivated.

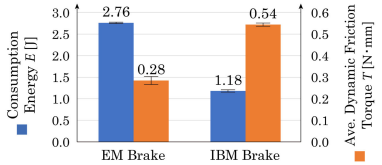

Fig. 17. Ten-time average dynamic friction torques exerted between the brake pads and consumption energy required to apply the brake pads for 1.0 s.

The examples of transitions of power consumption, dynamic friction torque, and rotation speed of the IBM brake and EM brake are compared as shown in Fig. 16. The graph clarifies the difference in the timing of the brakes to consume electricity: the EM brake requires constant consumption and the IBM brake consumption shows spikes at the beginning and end of braking. The IBM brake generated an apparently larger dynamic torque than the EM brake while using identical brake pads, which resulted in a larger deviation of the motor speed that emerges when activated and deactivated.

Fig. 17 contrasts the results of the dynamic experiment. The IBM brake generated a dynamic friction torque increased to 192.9% of the EM brake; however, it required only 42.8% power consumption. The torque–energy ratio is then increased to be 8.73 times, indicating that the proposed brake accomplished high performance in both braking torque and energy efficiency, for both holding an idling object and braking a rotating object.

The comparisons were made under the condition of applying brakes for 1.0 s. However, they can be expanded to any braking duration t; The theoretical energy consumption values of the EM brake E_{EM} and IBM brake E_{IBM} are calculated as

$$E_{\mathrm{EM}(t)} = 24.0\,[\mathrm{V}] \times 0.115\,[\mathrm{A}] \times t\ [\mathrm{s}] = 2.76t\,[\mathrm{J}] \quad (4)$$

$$E_{\mathrm{IBM}} = 0.59\,[\mathrm{J}] \times 2 = 1.18\,[\mathrm{J}] \quad (5)$$

Solving $E_{\mathrm{EM}(t)} \geq E_{\mathrm{IBM}}$ gives $t \geq 0.43$ s, which means that the proposed IBM brake with current constitution exceeds the energy performance of the EM brake with identical brake pads under any condition of continuous braking time longer than this t (or less frequent than $1/t = 2.3$ Hz); further, it surpasses in the generation of braking torque because of the pressing force amplification effect caused by the compensation. This implies that the IBM brake would not generate a tremendous amount of heat even when braking for a long time. Therefore, the IBM brake can be used in a variety of applications, to which the use of conventional EM brakes has been inadequate owing to the duty cycle. For example, 72% of cars in Japan wait for the signal crossing for 5 s on average [26], sufficiently long for the EM brake used in this research to heat up.

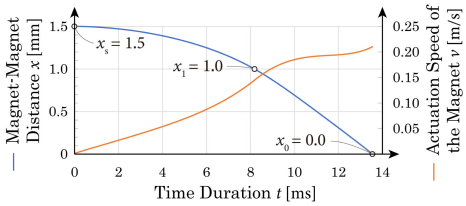

Fig. 18. Numerically analyzed transitions of the distance between the magnets and the actuation speed of the control rod of the proposed IBM brake.

VI. Discussion

A. Responsiveness of Braking

For the 2nd prototype of the IBM brake, the excitation time of the solenoid was empirically set to $14.0\ \mathrm{ms}$, which is the shortest duration for a stable behavior in any posture wherein the rotation axle of the system lies horizontally; the maximum duty cycle becomes $35.7\ \mathrm{Hz}$. If the current was applied for less than this duration, the control rod could not be fully pushed in and the magnets did not meet, which resulted in a forced deactivation of the brake. A numerical analysis was conducted to evaluate the reasonability of this responsiveness.

Let time T required for the self-holding solenoid to maintain its permanent magnetic flux cancelled out by the electromagnet equal the time required for the control rod to reach a stroke X (distance from x_s); the integration of the control force F_c on the control rod with a mass $m = 400\ \mathrm{g}$ gives its speed v as calculated below, where $x_{(t\,=\,0)} = v_{(t=0)} = 0$.

$$\int_0^X F_{\mathrm{c}(x)}\mathrm{d}x = \int_0^T m\ddot{x}\frac{\mathrm{d}x}{\mathrm{d}t}\,\mathrm{d}t = \int_0^T mv\,\mathrm{d}t$$

$$= \left[\frac{1}{2}mv^2\right|_0^T = \frac{1}{2}m\left(v_{(T)}^2 - v_{(0)}^2\right) \tag{6}$$

$$\Rightarrow\ v_{(t)} = \sqrt{\frac{2}{m}\int_0^{X_{(t)}} F_\mathrm{c}\mathrm{d}x} \tag{7}$$

Given the speed of the rod at time moment $\mathrm{n}\Delta t\ (\mathrm{n} = 1, 2, \ldots)$, an iterative calculation yields the required n for the x to reach x_s at the end of the stroke.

$$x_{(\mathrm{n})} \cong x_{(\mathrm{n}-1)} + v_{(\mathrm{n})}\Delta t \tag{8}$$

As plotted in Fig. 18, the transition of the displacement and speed of the control rod were numerically derived with $\Delta t = 50\ \mu\mathrm{s}$ (defined considering the significant digits), and the duration T to reach x_s was $13.6\ \mathrm{ms}$. The delay in the empirical value may have resulted from friction in the translational movement of the control rod. The inertias of the springs and their connection point (active brake pad in this mechanism) also could have affected the responsiveness because the multistage spring was designed using the synthesis of springs in series assuming they are negligible, whereas they do have mass in reality, as listed in Table II. Now that the performance comparison is done, the massive brake pad (of the EM brake, currently) can be replaced with a specifically dedicated design without unneeded structures such as a coil, both to improve the responsiveness and to reduce the gravitational disturbance on compensation, as discussed in the next subsection.

B. Effect of Gravity

The control force and friction torque were measured in a controlled situation such that the effect of the mass of moving parts on the translational pressing force between the brake pads could be ignored; the compensation spring was designed such that the minimization of the difference between the magnetic attractive force and spring repulsive force was the priority.

Although the experiments sufficiently proved the concept of the IBM brake, brakes can be installed in any orientation in practical applications, and the posture of the belonging mechanism can vary when applied to locomotive machines such as vehicles, robots, and robotic arms. Therefore, not only weight saving by the miniaturization of the structure but also selecting an actuator with a margin to obtain the weight of the control rod, designing the compensation spring with force bias against the known gravity direction, and combining a weight compensation mechanism should be considered for use in the actual environment.

C. Selection of Actuators

A simple self-hold solenoid was selected as an actuator to drive the brake, and experiments with dynamic performance were conducted only in a binary state of braking: activated and deactivated. However, as shown in Fig. 5, the intervention of the spring allows the pair of magnets to be separated from each other at an arbitrary distance. Therefore, other actuators with weak and short-stroke output but with more detailed positioning ability, such as artificial muscles made of shape-memory alloy, make it possible for the IBM brake to adjust the output braking torque in a more analog (or stepless) manner.

The constitution using an electromagnet (that contains a PM for self-holding feature) to shift the position of a PM may affect the compensation precision if they are aligned closely enough for their magnetic fluxes to interfere with each other. Therefore, if considering miniaturization, it shall be more simplified and evolved into an EPM relation. Hints for further improvement may lie in solenoid actuators with internal force compensation; there are solenoid valves with an embedded PM that use two-staged return springs to provide two flow rates or states of open and close using one degree of freedom selectively [27], [28]. Still, while they are specified as EPM actuators, the way an IB magnet is used in the proposed brake mechanism is categorized as a reduction mechanism that does not restrict the actuator to drive. Therefore, it can be activated even without electricity by human power as a tool or by an external mechanical force in the environment as a passive (load-sensitive) mechanism.

D. Design of Multistage Spring

In addition to the attractive force of the pair of PMs, linear springs also have their own deviation of spring constants and free lengths from their catalog values. The 2nd prototype of the IBM brake in this research absorbed by these errors insert a few shim rings; however, it took an unreasonably long time to determine the best adjustment as it required partial disassembly every time. For the easier adjustment of the spring independent of its individual difference considering a mass production in the future, another multistage spring made of a single coil spring split in two by a connector can be composed, as shown in Fig. 19. A spiral slit is engraved on the connector so that it can slide up and down on the wire of the spring, while re-defining the spring constants (numbers of active coils) of the two split springs. Weakening the suspension spring also allows the brake pads to be realigned for reduced pad wear.

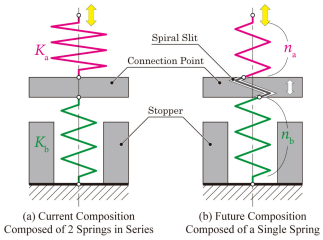

Fig. 19. Concept of the multistage springs composed of (a) Two linear springs proposed in this research and (b) a single coil spring split in two by a connector.

VII. Conclusion

We proposed the concept of an IBM brake and built the 1st prototype for POC. Experiments were conducted to verify the amplification feature of its magnets on the braking torque and the compensation feature of its spring on the input control force. The prototype demonstrated that the torque–force ratio was at most 18.1 times that of the contrasted EM brake. Further, the difficulties in using a conical coil spring, that is, restriction in characteristic design, inconvenience in production, and a long actuation stroke required for pad separation, were discussed.

To overcome these problems, a novel nonlinear spring comprising two linear springs in series was devised. One spring works for compensating and the other for suspending the brake pads, while they serve as a single synthesized compensation spring when brake pads are separated; this resulted in switching the spring constant to follow the nonlinearity of the attractive force of magnets. A 2nd prototype using this multistage spring was developed and verified to be effective; in particular, the dynamic torque increased to 192.9% that of the EM brake while consuming energy only when latching the braking state, resulting in a higher torque–energy efficiency when braking longer than 0.43 s. The numerical calculation results confirmed that the observed responsiveness of the brake was in line with the theoretical value and comparable to the existing EM brake.

In this manner, the proposed principle of the IBM brake was successfully validated, implying that replacing conventional EM brakes with the IBM brakes would contribute to a significant increase in mileage of vehicles and reduction in electricity costs of robotic arms in production lines, as intended in the research. Furthermore, the multistage spring alone would also be effective in shortening the stroke of an IB magnet, used for applying attractive force toward walls and ceilings, in exchange for partial reduction in attraction force.

In future studies, we intend to adopt mechanisms to improve the structural design left unsophisticated. A multistage single spring will be considered for achieving higher compensation precision with an easier adjustment method, along with a weight compensation mechanism to make the brake orientable to any installation posture. In addition to replacing EM brakes, the application is expanded to the study of robotic components such as EM clutches and parallel grippers that can amplify the translational force of a weak, short-stroke actuator.

References

[1] F. Flemming, "The basics of electromagnetic clutches and brakes," *Mach. Des.*, pp. 55–58, Jul. 9, 2009.

[2] C. Xiang *et al.*, "Experiment, optimization, and design of electromagnetic track brake for high-speed railways system," *Math. Problem Eng.*, vol. 2020, 2020, Art. no. 6957963.

[3] M. Zhileykin and G. Skotnikov, "The method of increasing the stability of trailer-trucks in case of emergency braking in a turn and emergency failure of the trailer brake system," *Proc. IOP Conf. Ser. Mater. Sci. Eng.*, vol. 820, no. 1, 2020, Art. no. 012017.

[4] J. L. Liu, S. K. Wang, and J. Z. Wang, "The experimental research of magnetic powder brake loading characteristic in rotary system," *Appl. Mech. Mater.*, vol. 130–134, pp. 3237–3241, 2012.

[5] W. H. Li and H. Du, "Design and experimental evaluation of a magnetorheological brake," *Int. J. Adv. Manuf. Technol.*, vol. 21, no. 7, pp. 508–515, 2003.

[6] J. Nadeau, M. Boisvert, and P. Micheau, "Implementation of a cooperative strategy between a vehicle's mechanical and regenerative brake system," in *Proc. IEEE Veh. Power Propulsion Conf .*, 2014, pp. 1–6.

[7] T. Zalud, "Getting a grip on clutch and brake selection," *Mach. Des.*, vol. 71, no. 17, pp. 83–86, 1999.

[8] Z. Ansari *et al.*, "Design and development of electro magnetic braking system," *Int. J. Eng. Res.*, vol. 6, no. 4, pp. 314–320, 2017.

[9] J. Kim and J. Chang, "A new electromagnetic linear actuator for quick latching," *IEEE Trans. Magn.*, vol. 43, no. 4, pp. 1849–1852, Apr. 2007.

[10] Y. P. Yang *et al.*, "Multifunctional optimal design of an electromagnetic valve actuator with hybrid magnetomotive force for a camless engine," in *Proc. Int. Conf. Electron. Mach. Syst.*, 2011, pp. 1–6.

[11] B. V. Ravi Kumar *et al.*, "Design of a new electromagnetic brake for actuator locking mechanism in aerospace vehcile," *IEEE Trans. Magn.*, vol. 53, no. 11, Nov. 2017, Art no. 8002606.

[12] T. Shimizu *et al.*, "MR fluid jamming gripper applying internally-balanced magnetic unit controllable by small control force," in *Proc. JSME Annu. Conf. Robot. Mechatronics*, 2019, pp. 2A2–G03.

[13] T. Shimizu *et al.*, "Small swarm search robot system with rigid-bone parachute rapidly deployable from aerial vehicles," in *Proc. IEEE Int. Symp. Saf., Secur., Rescue Robot.*, 2019, pp. 88–93.

[14] T. Shimizu *et al.*, "Internally-balanced magnetic mechanisms using a magnetic spring for producing a large amplified clamping force," in *Proc. IEEE Int. Conf. Robot. Automat.*, 2020, pp. 1840–1846.

[15] V. Arakelian, M. Dahan, and M. Smith, "A historical review of the evolution of the theory on balancing of mechanisms," in *Proc. Int. Symp. Hist. Mach. Mechanisms Proc.*, 2000, pp. 291–300.

[16] T. Aibara *et al.*, "Development of a portable field arm with gravity compensation," in *Proc. JSME Annu. Conf. Robot. Mechatronics*, 2008, pp. 1A1–H01.

[17] S. Hirose *et al.*, "Internally balanced magnetic unit.," *J. Robot. Soc. Jpn.*, vol. 3, no. 1, pp. 10–19, 1985.

[18] K. Tadakuma and T. Tanaka, "IBM wheel: Mechanism of internal balanced magnetic wheel: Basic concept and the first prototype model," in *Proc. JSME Annu. Conf. Robot. Mechatronics*, 2014, pp. 1P2–O01.

[19] M. Ozawa *et al.*, "Internally balanced magnetic crawler," in *Proc. 19th Annu. Conf. Syst. Integr. Division Soc. Instrum. Control Eng.*, 2017, pp. 1D5–108.

[20] K. Yanagimura *et al.*, "Hovering of MAV by using magnetic adhesion and winch mechanisms," in *Proc. IEEE Int. Conf. Robot. Automat .*, 2014, pp. 6250–6257.

[21] S. Murata *et al.*, "M-TRAN: Self-reconfigurable modular robotic system," *IEEE/ASME Trans. Mechatronics*, vol. 7, no. 4, pp. 431–441, Dec. 2002.

[22] *Electromagnetic Clutches and Electromagnetic Brakes—Part 2: Test Methods*, Japanese Industrial Standards B1404-2-2005, 2005.

[23] M. Suzuki, K. Tsuru, and S. Hirose, "Design of nonlinear spring and mechanism for internally-balanced magnetic unit," *J. Robot. Soc. Jpn.*, vol. 27, no. 4, pp. 460–469, 2009.

[24] K. Nagaya *et al.*, "Low driving energy engine valve mechanism using permanent-electromagnet and conical spring," *Int. J. Appl. Electromagn. Mech.*, vol. 28, no. 1/2, vol. 47683, pp. 267–273, 2008.

[25] R. C. Redfield, "Design parameter sensitivity for a mountain bike rear shock," *Amer. Soc. Mech. Eng. Dyn. Syst. Control Division DSC*, vol. 47683, pp. 1167–1174, 2007.

[26] K. Mori and M. Taniguchi, "A study on the influence of the idling stop at signals on the traffic smoothness," *Infrastructure Plan. Rev.*, vol. 24, pp. 775–780, 2007.

[27] K. E. Beyer and W. H. Horlacher, "Two-stage solenoid valve," U.S. Patent US4546955A, Oct. 14, 1982.

[28] F. Fuchs, "Solenoid valve," U.S. Patent US5029807A, Apr. 30, 1990.